



# Feasibility study for the manufacturing of hybrid pinion shafts with the cross-wedge rolling process

Paulina Merkel<sup>1</sup> · Laura Budde<sup>2</sup> · Jan Grajczak<sup>2</sup> · Christian Nowroth<sup>3</sup> · Vannila Prasanthan<sup>4</sup> · Mareile Kriwall<sup>1</sup> · Marius Lammers<sup>2</sup> · Sarah Nothdurft<sup>2</sup> · Jörg Hermsdorf<sup>2</sup> · Jens Twiefel<sup>3</sup> · Ludger Overmeyer<sup>2</sup> · Stefan Kaierle<sup>2,5</sup> · Jörg Wallaschek<sup>3</sup> · Bernd Breidenstein<sup>4</sup> · Bernd-Arno Behrens<sup>1,6</sup> · Malte Stonis<sup>1</sup>

Received: 29 September 2022 / Accepted: 9 May 2023 / Published online: 7 July 2023  
© The Author(s) 2023

## Abstract

The Collaborative Research Center 1153 is investigating an innovative process chain for the production of hybrid components. The hybrid workpieces are first joined and then formed by cross-wedge rolling. Pinion shafts were manufactured to investigate the behavior of the joining zone under increased complexity of the forming process. For this purpose, six types of workpieces produced by three types of joining processes were formed into pinion shafts. The reference process provides a shaft with a smooth bearing seat. It was found that the increased complexity did not present any challenges compared to the reference processes. A near-net shape geometry was achieved for the pinions made of steel.

**Keywords** Hybrid components · Cross-wedge rolling · Hot forming · Laser beam welding · Laser hot-wire deposition welding

## Introduction

When it comes to meeting the requirements in transmission construction, monomaterials reach their limits. Increasing technical requirements as well as rising costs due to material shortages further aggravate the problem of material selection [1]. Hybrid components are suitable for extending the application limits and increasing resource efficiency. The Collaborative Research Center (CRC) 1153 is researching the "Tailored Forming" process chain for manufacturing hybrid components. The combination of aluminum and steel leads to a reduction in component mass while retaining the properties of steel in relevant areas of the component. Hybrid components made of two or more steel grades enable withstanding high load capacities by integrating a corresponding material in the relevant zone while saving alloying elements in the rest of the component. Hence, the component is adapted according to the load profile [2].

One forming process used in the CRC 1153 is the cross-wedge rolling (CWR) process. CWR is a preform operation used to increase resource efficiency [3]. It is an incremental forming process that produces rotationally symmetrical workpieces. Two tools move in opposite directions and reshape the workpiece located in between [4]. The tools are equipped with a wedge profile that forms the workpiece. The wedges are profiled with serrations to ensure sufficient friction between workpiece and tool. The principle of the tool construction is shown in Fig. 1. The tool is divided into three zones: knifing zone, stretching zone and sizing zone [3]. In the knifing zone, the wedge first sinks into the workpiece [3]. The workpiece is then further formed in the stretching zone of the tool [3]. Finally, the workpiece is calibrated in the sizing zone and the noses caused by the serrations as well as other shape irregularities are removed [3]. The tools used for CWR in the CRC 1153 are modular in design. The sizing zone can be exchanged for an endpiece that forms pinions in the area of the bearing seat (see Fig. 8). In this way it is possible to form pinion shafts with the CWR process.

The motivation for examining a geometry with an increased complexity is to obtain general statements on process windows for the forming of hybrid workpieces. The CWR process is mainly influenced by the forming angle  $\alpha$ , the wedge angle  $\beta$  and the cross section reduction  $R_p$  [5].

---

Paulina Merkel, Laura Budde and Jan Grajczak contributed equally to this work.

✉ Paulina Merkel  
merkel@iph-hannover.de

Extended author information available on the last page of the article

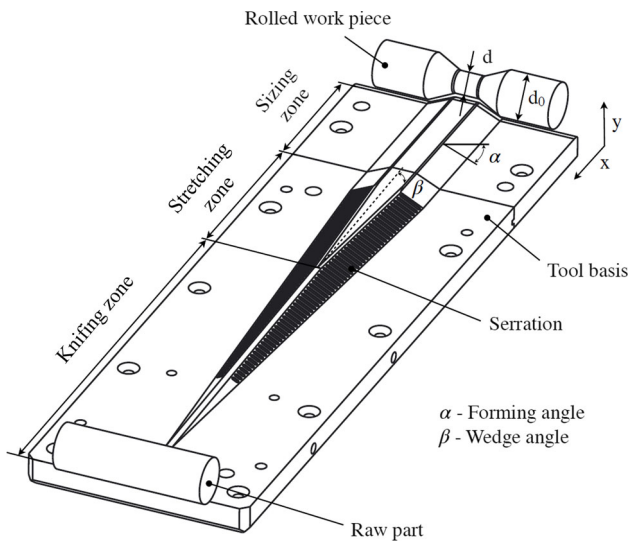


Fig. 1 Principle of the CWR tool, according to [3]

Since high cross section reductions (above 70%) are already challenging for mono-material components, this poses a particular difficulty with respect to the joining zone stability of hybrid workpieces [3]. By forming hybrid pinion shafts it is being investigated what maximum degrees of forming can be reliably formed in the area of serial joining zones or coaxial application by means of CWR without damaging the joining zone.

A pinion shaft is a combination of a gear and a drive shaft. It is used for a variety of gears in mechanical and plant engineering if the transmission ratio at high torques is critical due to small sizes of the gear [6]. Pinion shafts are often manufactured by forging, machining or rolling [7]. The positive effects of forming processes, such as grain refinement and adapted fiber courses, are then lost [8]. In addition, the

Fig. 2 Workpieces used for feasibility study

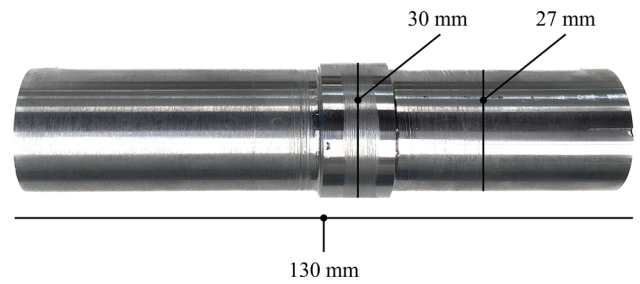
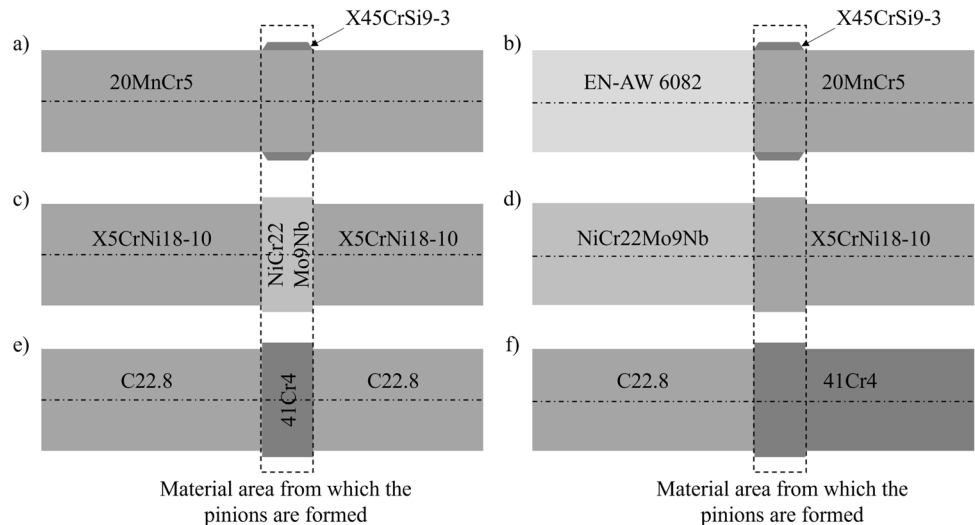


Fig. 3 Measurements of workpieces before cross-wedge rolling

resource efficiency is lower if the manufacturing process only consists of machining.

The aim of this work is to develop a stable forming process for hybrid pinion shafts and to design tools that form near-net shape. Six different types of workpieces are investigated. These workpieces are manufactured using three different joining processes and subsequently formed using the CWR process. The pinion shafts are then 3D-measured and compared to the optimal geometry.

### Manufacturing of hybrid workpieces

The hybrid workpieces are produced using deposition welding, laser beam welding and friction welding. The material combinations used are presented in Fig. 2. The dimensions of the workpieces are shown in the Fig. 3. For comparability, workpieces c)-f) were turned to have the same dimension as the workpieces a) and b). Workpiece a) is produced with deposition welding. Workpiece b) is produced by friction welding of aluminum and steel and the subsequent deposition welding of the cladding. Workpieces c) to f) are produced using laser beam welding.

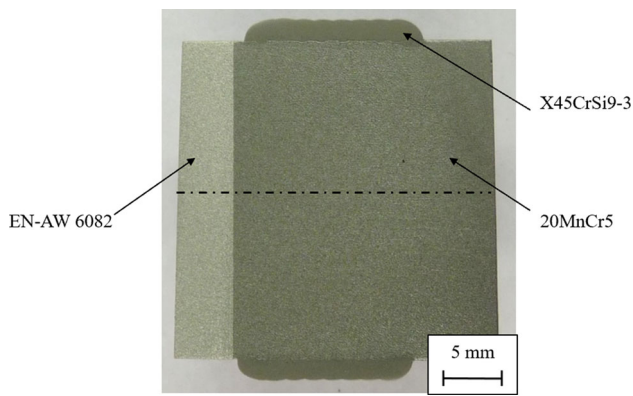


**Fig. 4** Cross section of workpiece b), manufactured by friction welding and laser hot-wire deposition welding

Hybrid components have several advantages, which are reflected in the workpieces used. Workpiece a) allows the use of a lower cost base material while maintaining the required properties of the pinions by using a higher alloyed material in this area. The cladding material takes up roughly 2% of the total volume of the workpiece. Thereby, the amount of highly alloyed material can be largely reduced whilst maintaining the necessary properties in the area of the pinions. Workpiece b) adds weight reduction to the list of advantages through the partial use of aluminum as the base material. The weight of the component can be reduced by 33%. Workpieces c) and d) allow the cost of the workpiece to be reduced while maintaining relevant properties such as durability at high temperatures and chemical resistance. Workpieces e) and f) are another example of the reduced use of high-alloy steels. In the case of workpieces c) and e) the area from which pinions are formed takes up 12% of the total volume. Workpieces d) and f) divide into 49% of NiCr22Mo9Nb or respectively C22.8 and 51% of X5CrNi18-10 or 41Cr4. This usage of differ-

ent materials can lead to a higher resource efficiency of the produced components.

**Deposition welding**

The claddings are applied using a laser hot-wire deposition welding process. A laser beam source with a wavelength of  $1,020$  to  $1,060 \pm 15$  nm and the coaxial deposition welding head MK-II, manufactured by Laser Zentrum Hannover e.V., is used for this purpose. Two layers of spiral weld seams are applied on the 20MnCr5 base material. In the case of workpiece b) the cladding is positioned close to the joining zone. The cladding has a height of 1.75 mm (workpiece b) or 1.92 mm (workpiece a) and a width of 15 mm. A cross section of a workpiece type b) can be seen in Fig. 4. The welding parameters used are shown in Table 1. The stickout is defined as the distance between the welding nozzle and the workpiece.

**Friction welding**

Serially arranged workpieces (workpiece b)) made of aluminum (EN-AW 6082) and steel (20MnCr5) are produced using the friction welding process at the Institute of Forming Technology and Machines, Hanover [9]. In this process, the workpieces are pressed together and rotated against each other. The friction between the two parts generates heat [10]. In conjunction with the pressure, the material is melted and a material bond is created between the joining partners [10].

**Laser beam welding**

Serially arranged workpieces made from NiCr22Mo9Nb and X5CrNi18-10 as well as the steel combination of C22.8 and

**Table 1** Welding parameters for laser hot-wire deposition welding of X45CrSi9-3 on 20MnCr5

Parameter	Unit	Workpiece b Value	Workpiece a Value
Welding speed	mm/min	1,200	1,000
Electric current			
- first layer	A	120	90
- following layers	A	120	80
Laser beam power	kW	1.5	2.1
Wire feed rate	m/min	2.4	2.0
Shielding gas flow rate (Argon)	l/min	8	6
Stickout	mm	5.7	6.9
Seam-to-seam offset	mm	1.6	1.6
Collimation length	mm	63	100
Optical fiber diameter	$\mu$ m	400	400
Focal length	mm	300	300
Spot diameter	mm	3.1	3.0

**Table 2** Specifications of laser beam welding setup

Parameter	Unit	Value
Wavelength	nm	1,030
Optical fiber diameter	$\mu\text{m}$	200
Collimation length	mm	150
Focal length	mm	300
Focal spot diameter	$\mu\text{m}$	400

41Cr4 are produced using the laser beam welding process at the Laser Zentrum Hannover e.V. During circumferential laser beam welding the specimen is rotated and the processing head is stationary. To prevent melt drop formation, the processing head is angled by  $20^\circ$ . Argon shielding and process gas is provided by two flat nozzles below and above the specimen for cooling, melt drop prevention and gas plume reduction. For clamping, a setup for ultrasonic assisted laser beam welding with a clamping pressure of 200 bar is used. More parameters are shown in Tables 2 and 3. A cross section of a laser beam welded specimen is shown in Fig. 5. It shows two seams with pores in the center, which were created by the welding process. The cause of these pores is that the welding depth was exaggerated. The specimen shown is a reject specimen.

## Forming of hybrid workpieces

The CWR experiments were conducted using the CWR module at the IPH - Institut für Integrierte Produktion Hannover gGmbH. The tool speed was set to 150 mm/s. The tools were preheated to  $150^\circ\text{C}$  to reduce temperature loss from the workpiece during forming. The workpieces were heated using an induction heating unit by EMA-TEC GmbH.

Forming depends largely on tool parameters (Fig. 1), but also on material and temperature properties [3] [11]. For hybrid material forming processes the forming parameters of different materials have to be matched to each other. Therefore, the yield stresses of materials are compared. The yield stresses of aluminum and steel at a homogeneous forming temperature vary strongly [11]. Accordingly, hybrid workpieces made from steel and aluminum (workpiece b)) are

**Table 3** Parameters of laser beam welding

Parameter	Unit	Value
Gas flow rate	l/min	60
Defocusing	mm	-4
Laser beam power	kW	8
Welding speed	m/min	0.95

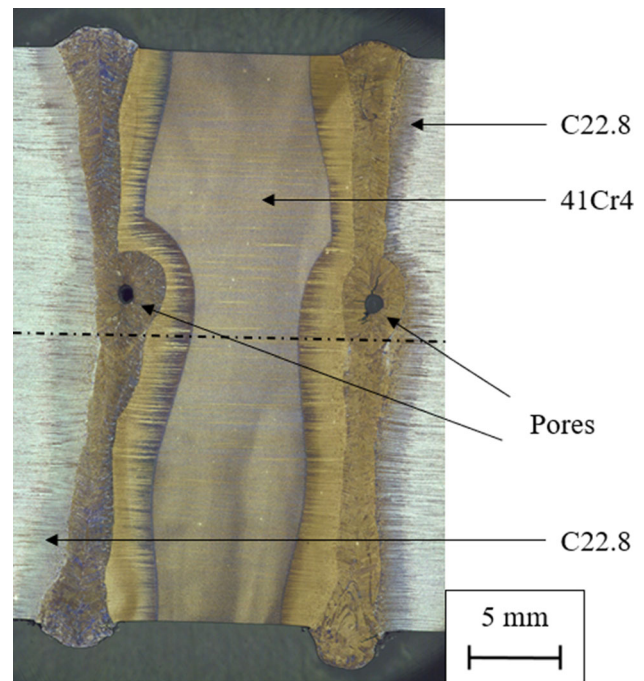


**Fig. 5** Cross section of a laser beam welded workpiece e) made from 41Cr4 and C22.8

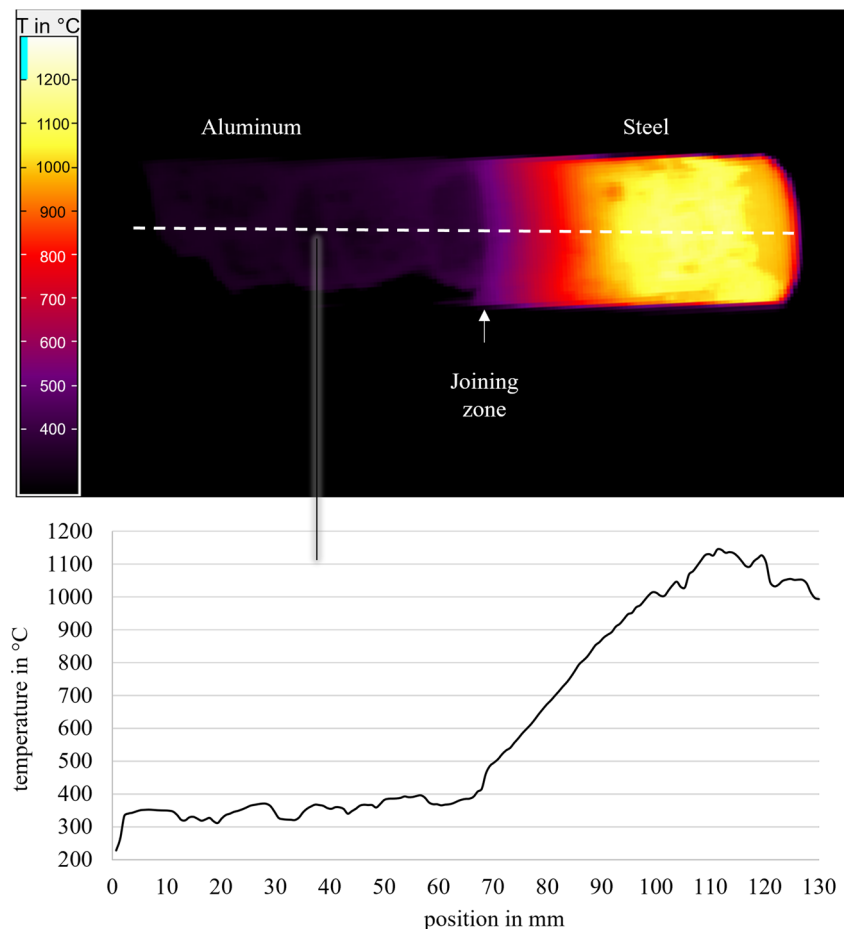
partially heated to create an inhomogeneous temperature distribution [11]. The steel side is heated using the induction heating unit. The aluminum is heated by the conduction of heat from the steel side. This results in a temperature distribution as seen in Fig. 6. The temperature distribution was measured using a thermal imaging camera. The temperature on the steel side is a maximum of  $1,100^\circ\text{C}$  and the aluminum side is an average temperature of  $380^\circ\text{C}$ . The temperature distribution causes yield stresses of the two materials that are adapted to each other.

Workpieces a), e) and f) were heated to  $1,250^\circ\text{C}$  homogeneously. Workpieces c) and d) were heated to  $1,080^\circ\text{C}$ . The temperature distribution of workpiece d) was measured using a thermal imaging camera (Fig. 7). The results show a mostly homogeneous temperature distribution with end pieces that are cooled down more than the rest of the workpiece. The deviations of the graph (especially in the area of the joining zone) can be explained by deviating emissivities in the respective areas.

## Production of pinion shafts

Pinion shafts are produced by forging, machining or rolling [7]. In this paper, the possibility of using CWR is investigated. The tools are designed according to the Roto-Flo-Process [4]. The tool is divided into three zones: knifing, stretching and sizing zone (see Fig. 1). In the case of the reference

**Fig. 6** Temperature distribution in serially arranged aluminum-steel workpieces measured with a thermal imaging camera



process, the sizing zone forms a smooth bearing seat. For the production of pinion shafts the end piece of the CWR tool (the sizing zone) is exchanged for an end piece which forms pinions in the area of the bearing seat. The molds for forming the pinions are developed in accordance with literature [12]. The geometry of the pinion mold can be seen in Fig. 8. This tool creates a straight-toothed gear as seen in Fig. 9.

## Results

Different workpieces were manufactured and cross-wedge rolled to determine the feasibility of producing hybrid pinion shafts with the CWR process. For reference, each material combination was also examined without the formation of pinions, i.e. with a smooth bearing seat. The hybrid pinion shafts were then measured using an optical 3D-measurement system (GOM ATOS Core 80). The measured surfaces were compared to the target geometry in Fig. 9.

### Workpiece a)

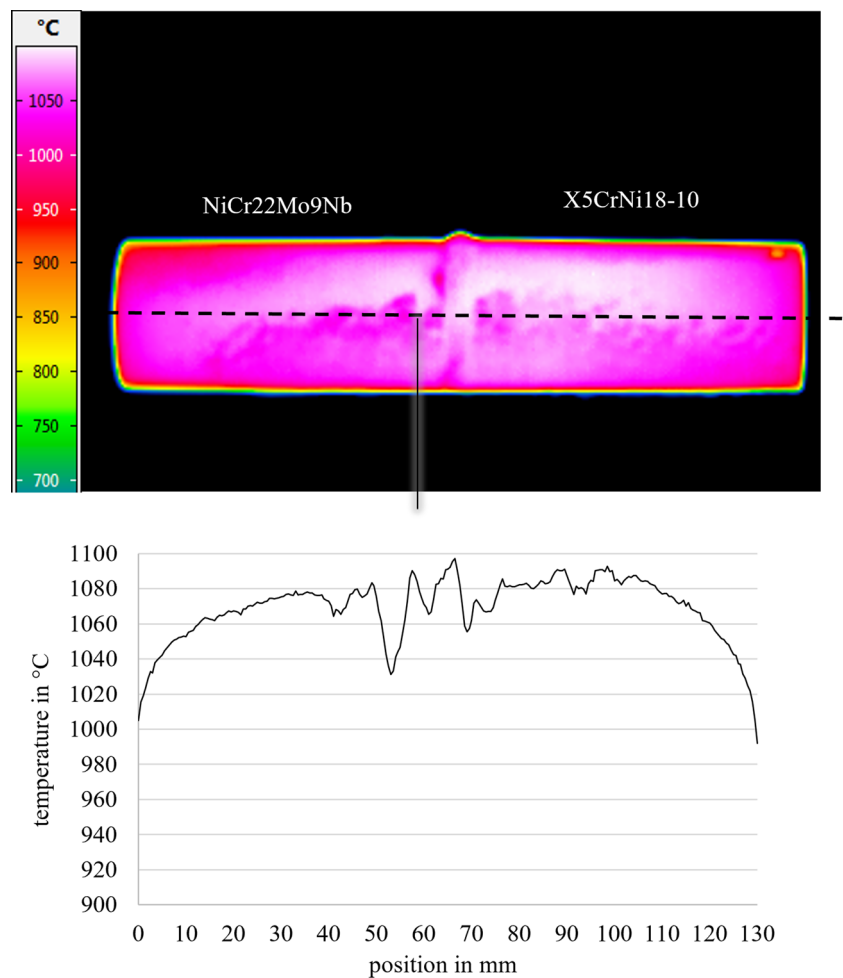
In a previous study, it was found that the material combination of 20MnCr5 and X45CrSi9-3 is suitable to produce hybrid

workpieces with a smooth bearing seat [13]. In this study two workpieces made from this material combination were formed into pinions. The cladding was successfully formed into pinions without layer separation. The distribution of the cladding after forming can be seen in Fig. 10. The pinions are fully coated with cladding. It was also found that the gaps between the pinions have sufficient coverage with the protective layer of cladding.

The material exhibits core loosening, also known as the Mannesmann effect. This involves the formation of cavities in the center of a shaft due to stresses in the CWR process [14]. Former studies show that this is most likely caused by the high sulfur content in 20MnCr5 [15]. Cavities also occurred in the reference process. The cavities increase the volume of the shaft in that area and cause ovalization on the right hand side of the pinion shaft.

In Fig. 11 the 3D-measurement of the formed pinion shaft is visible. The colors indicate how much the shaft deviates from the target geometry. The target geometry show the pinion shaft after machining. It is therefore crucial that the deviation is on the positive side to ensure that there is sufficient material for machining. 68.3% of the measurement points that fit the target geometry best were considered. This

**Fig. 7** Thermal imaging camera measurements of a serially arranged NiCr22Mo9Nb-X5CrNi18-10 workpiece after induction heating



corresponds to a sigma of all points. Considering a higher number of points is not suitable due to the resolution of the 3D measurements. On the right side the formed shaft deviates a lot from the target geometry due to the ovalization. The deviations in the area of the pinions averages 1.03 mm. Smaller areas with a high deviation of -4.00 mm are visible. These are most likely caused by gaps in the 3D-profile of the formed pinion shaft.

### Workpiece b)

Workpiece b) could not be formed into a pinion shaft. The workpieces broke during CWR right before the sizing zone. This could be due to the fact that the cladding layer was welded too close to the weld seam between aluminum and

steel. This means that the thermal influence on the joining zone during the welding process was too high. In a reference process, a shaft made of the same three materials had already been successfully cross-wedge rolled. For this workpiece, there was a space of about 3 mm between the aluminum and steel joining zone and the start of the cladding. The other possible cause is that the temperatures during cross-wedge rolling were too high. In order to rule out this possibility, several experiments were carried out at lower temperatures. Even at lower average temperatures the joining zone came loose.

In order to characterise the subsurface, X-ray residual stress measurements were carried out using the  $\sin^2\psi$ -method with Cr  $K\alpha_1$  radiation with a fixed wavelength of 2.2897 Å. The measurements were conducted on a Seifert

**Fig. 8** Cross-section of the tool geometry

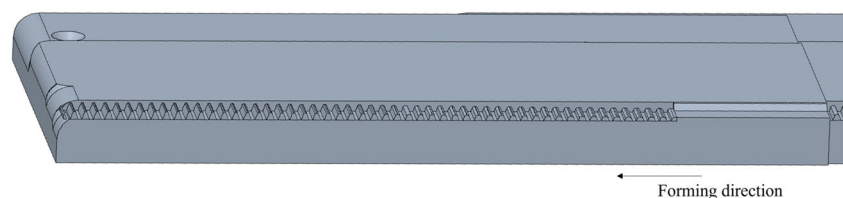
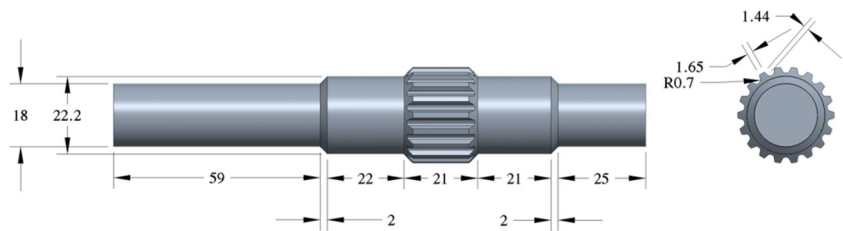


**Fig. 9** Target geometry of the hybrid pinion shaft after machining



XRD 3003TT two circle X-ray diffractometer. The measuring beam was limited by a 1 mm point collimator. The measurements identified compressive residual stresses of -410 MPa in the axial direction at the tip of the teeth. In literature, tensile residual stresses were measured at the tip of the teeth and large compressive residual stresses at the root of the teeth, which lead to an early failure [16]. Here, the tensile residual stresses at the tooth tip were listed as the cause for the premature failure of the pinion shaft. This means that in the produced hybrid shaft, the weak point with regard to the subsurface could be eliminated. In future work, a special focus will be placed on the detailed characterisation (residual stress depth profiles and locally resolved residual stress determination) of the subsurface and lifetime of these components.

### Workpiece c)

Workpiece c) could not be formed into a pinion shaft. On the side with the higher degree of forming (left sides of the workpieces in Fig. 2) the X5CrNi18-10 broke. To rule out errors in temperature control, experiments were carried out at other temperatures. At a temperature of 1,100 and 1,200 °C the joining zone between the serially arranged materials broke. To confirm that the degree of forming is limited for X5CrNi18-10 experiments using monolithic workpieces were performed. It was not possible to identify process

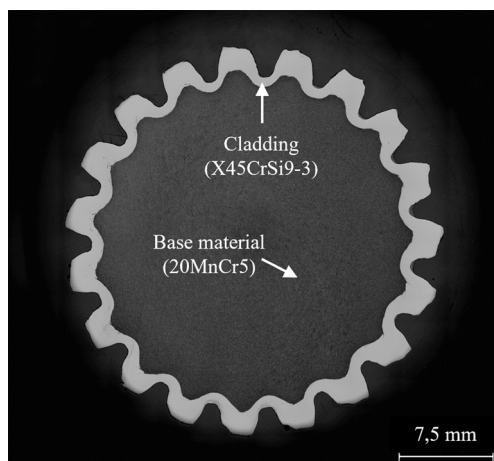


**Fig. 10** Cross section of a pinion shaft produced from workpiece a)

parameters (e.g. forming temperature, tool velocity) that would lead to defect free shafts. It is possible that a different tool geometry (e.g. different values for  $\alpha$  and  $\beta$ ) would lead to a defect free shaft. The pinions made of NiCr22Mo9Nb could be formed, but the tool was heavily worn by the toughness of the material. The tool is made from 55NiCrMoV7 and hardened to 52 HRC. The first signs of wear appeared after only 5 experiments. After 30 experiments with the material combinations mentioned in this paper, the tool was so heavily worn that no further experiments could take place. It is possible that forming at a higher temperature and with a further hardened tool would give better results with regard to the near-net shape production.

### Workpiece d)

Workpiece d) could be successfully formed into a pinion shaft. The contour of the pinions made of NiCr22Mo9Nb could be improved by using a harder tool. The tool wear in these experiments was extraordinarily high. For workpieces c) and d) it was found, that the wedge tip must not cut into one of the joining zones. If the wedge cut into the joining zone, the workpiece broke after just a few seconds of CWR. The 3D-measurement of a workpiece d) is visible in Fig. 12. As expected the pinions made from NiCr22Mo9Nb are less pronounced and show an average deviation of 1.13 mm from the target geometry in the area of the pinions. The average deviation is probably higher, but the quality of the obtained 3D-profile was low due to the glossiness of the formed pinion shaft.

### Workpieces e) and f)

Workpieces e) and f) were formed into pinion shafts without any defects. Figure 13 shows the part made from workpiece e) after turning. The 3D-measurement of workpiece f) can be seen in Fig. 14. It is visible, that the base material formed near-net shape. The pinions are formed with deviations of 1.42 mm on average to the target geometry. Although this is the largest deviation, the workpiece can be machined without defects as shown in Fig. 13.

Comparing all the 3D-measurements shows, that workpiece a) has the lowest average deviation from the target geometry. Small defects are visible in the pointed transition between the pinion and the rest of the shaft. Workpiece d)

**Fig. 11** Deviation from the target geometry of workpiece a)

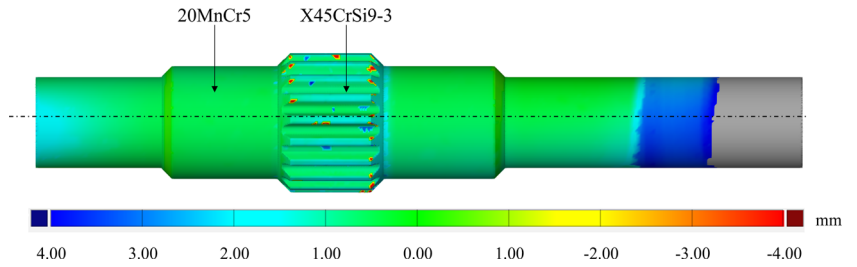


**Fig. 12** Deviation from the target geometry of workpiece d)

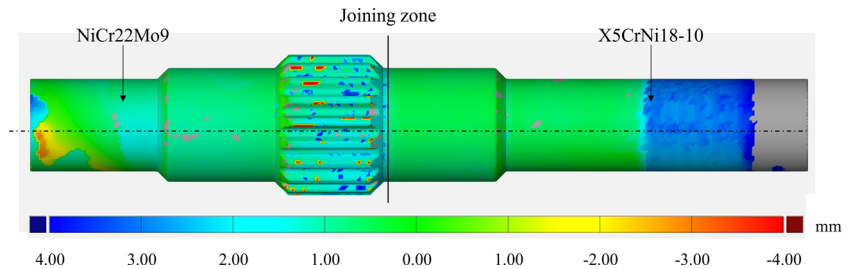


**Fig. 13** Workpiece e) after turning

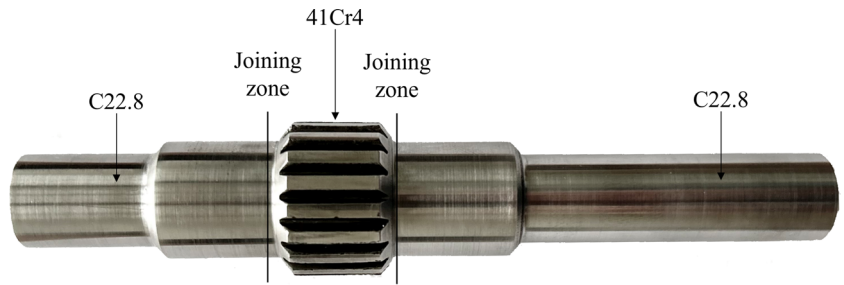


**Fig. 14** Deviation from the target geometry of workpiece f)

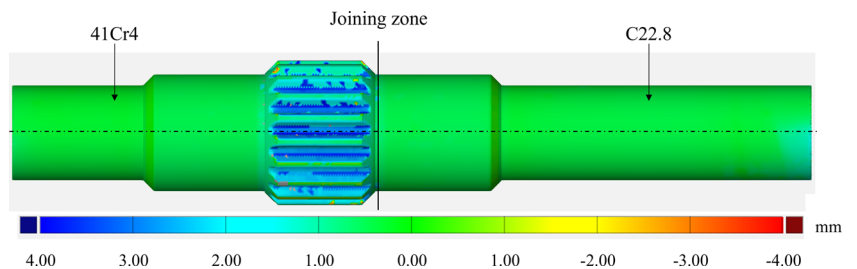
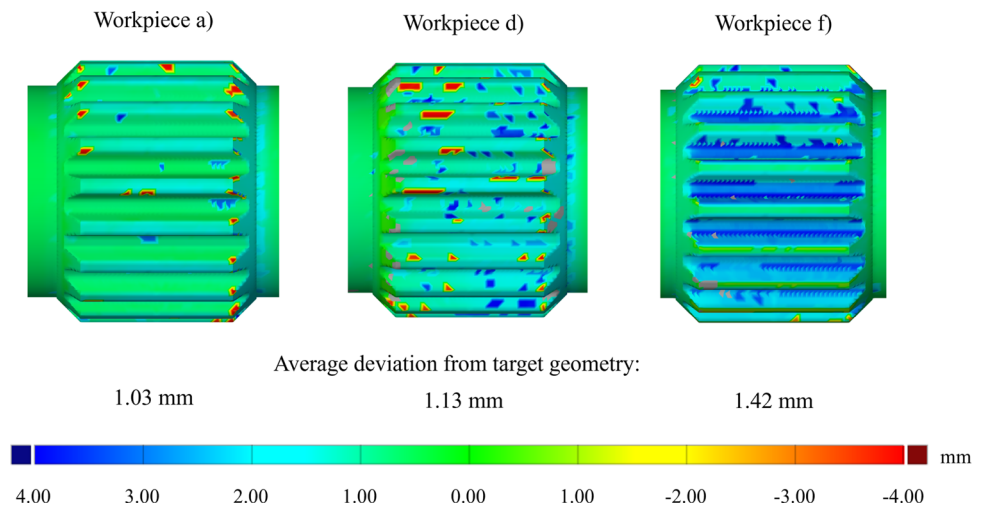


**Fig. 15** Comparison of deviations from the target geometry



shows a more inhomogeneous surface texture. Although the average deviation from the target geometry is only 1.13, the pinions were not fully developed as needed. Larger areas show deviations into the negative range, which would prevent successful machining. Workpiece f) shows a large average deviation of 1.42 mm. Since all deviations are in the positive range, a pinion shaft could be produced from this preform.

## Summary

- Workpieces a), e) and f) could be formed into hybrid pinion shafts without defects. A near-net shape was achieved.
- In the case of workpiece a) the pinions are formed entirely from cladding material, so that a good distribution of material can be assumed.
- It is possible to form NiCr22Mo9Nb and X5CrMo18-10 into pinions. The near-net shape could be improved by higher forming temperatures or a tool with increased hardness (e.g. by additional hardening of the tool teeth).
- The possible degree of forming for the material X5CrNi18-10 using the CWR process is limited.
- An increase in the forming temperature for NiCr22Mo9Nb-X5CrNi18-10 combinations leads to failure of the joining zone.
- To avoid material failure in NiCr22Mo9Nb-X5CrNi18-10 combinations, the wedge of the tool must not cut into the joining zone.
- The tool wear due to the experimental tests is high. Especially for serially arranged aluminum-steel workpieces due to the temperature distribution and for NiCr22Mo9Nb due to the low formability of the material.
- For workpieces made of three materials (EN-AW 6082, 20MnCr5 and X45CrSi9-3), the distance between the joining zone of friction welding and the start of cladding should be increased to reduce the influence of deposition welding on the intermetallic phase.

**Acknowledgements** This research was funded by the Deutsche Forschungsgemeinschaft (DFG, German Research Foundation)-CRC 1153, sub-projects A3, A4, B1, B3, B4-252662854

**Funding** Open Access funding enabled and organized by Projekt DEAL.

## Declaration

**Conflict of Interest for all authors** None

**Open Access** This article is licensed under a Creative Commons Attribution 4.0 International License, which permits use, sharing, adaptation, distribution and reproduction in any medium or format, as long as you give appropriate credit to the original author(s) and the source, provide a link to the Creative Commons licence, and indi-

cate if changes were made. The images or other third party material in this article are included in the article's Creative Commons licence, unless indicated otherwise in a credit line to the material. If material is not included in the article's Creative Commons licence and your intended use is not permitted by statutory regulation or exceeds the permitted use, you will need to obtain permission directly from the copyright holder. To view a copy of this licence, visit <http://creativecommons.org/licenses/by/4.0/>.

## References

1. Buchmayr B (2015) Aktuelle Entwicklungstrends und zukünftige Herausforderungen im Bereich der Umformtechnik. *Berg huettenmaenn monatsh* 160:501–506. <https://doi.org/10.1007/s00501-015-0402-1>
2. Behrens B-A, Uhe J, Petersen T, Klose C, Thürer SE, Diefenbach J, Chugreeva A (2021) Challenges in the forging of steel-aluminum bearing bushings. *materials* 14(4). <https://doi.org/10.3390/ma14040803>
3. Pater Z (2014) Cross-wedge rolling. *comprehensive materials processing* 4:211–279. <https://doi.org/10.1016/B978-0-08-096532-1.00315-0>
4. Hoffmann H, Neugebauer R, Spur G (2012) *Handbuch umformen*, Carl Hanser Verlag, München
5. Li Q, Lovell MR, Slaughter WS, Tagavi KA (2002) Investigation of the morphology of internal defects in cross wedge rolling. *Journal of Materials Processing Technology* 125:248–257
6. Gokcek M (2012) *Mechanical engineering*. Croatia, InTech. ISBN. 9535105051
7. Pater Z, Gontarz A, Tofil A (2011) Analysis of the cross-wedge rolling process of toothed shafts made from 2618 aluminium alloy. *Journal of Shanghai Jiaotong University (Science)* 16:162–166. <https://doi.org/10.1007/s12204-011-1119-2>
8. Doege E, Behrens B-A (2016) *Handbuch umformtechnik*. VDI-Buch. Springer, Berlin, Heidelberg. <https://doi.org/10.1007/978-3-662-43891-6>
9. Behrens B-A, Uhe J, Stier F, Duran D, Matthias T, Ross I (2021) Fabrication of steel-aluminium parts by impact extrusion. *Materials Today: Proceedings*. <https://doi.org/10.1016/j.matpr.2021.11.093>
10. Ambroziak A, Korzeniowski M, Kustron P, Winnicki M, Sokołowski P, Harapinska E (2014) Friction welding of aluminium and aluminium alloys with steel. *advances in materials science and engineering*. <https://doi.org/10.1155/2014/981653>
11. Behrens B-A, Chugreev A, Selinski M, Matthias T (2019) Joining zone shape optimisation for hybrid components made of aluminium-steel by geometrically adapted joining surfaces in the friction welding process. *AIP Conference Proceedings*, 2113, 040027. <https://doi.org/10.1063/1.5112561>
12. Hellfritsch U, Lorenz B, Quaas J (2004) *Werkzeug und verfahren zum querwalzen von verzahnungen sowie verfahren zur herstellung eines walzwerkzeuges*, google patents, DE 100 66 177 A1. <https://patents.google.com/patent/DE10066177B4/de>
13. Budde L, Biester K, Merkel P et al (2022) Investigation of the material combination 20MnCr5 and X45CrSi9-3 in the tailored forming of shafts with bearing seats. *Prod. Eng. Res. Devel.* <https://doi.org/10.1007/s11740-022-01119-w>
14. Wang M, Xiang D, Xiao C, Zhou J, Jia Z (2012) Influence of cooling condition of tools on central deformation of workpiece and tool wear in cross wedge rolling. *The International Journal of Advanced Manufacturing Technology*. <https://doi.org/10.1007/s00170-011-3537-6>

15. Idoyaga Z, Elvira R, Wendenbaum J, Meunier J, Robelet M, Toscanelli O, Reis M, Zachäus R, Lorenz B, Kolbe M (2008) Influence of tramp elements (P, Cu, S, Sn) on the mannesmann effect in the transversal hot rolling of engineering steels (MANNESTRAMP). Brussels: European Commission, Report of the Commission of the European Communities - EUR, Technical steel research, 23597
16. Rajinikanth V, Soni MK, Mahato B, Ananda Rao M (2019) Study of microstructural degradation of a failed pinion gear at a cement plant. *Engineering Failure Analysis*. <https://doi.org/10.1016/j.engfailanal.2018.08.031>

**Publisher's Note** Springer Nature remains neutral with regard to jurisdictional claims in published maps and institutional affiliations.

## Authors and Affiliations

Paulina Merkel<sup>1</sup>  · Laura Budde<sup>2</sup> · Jan Grajczak<sup>2</sup> · Christian Nowroth<sup>3</sup> · Vannila Prasanthan<sup>4</sup> · Mareile Kriwall<sup>1</sup> · Marius Lammers<sup>2</sup> · Sarah Nothdurft<sup>2</sup> · Jörg Hermsdorf<sup>2</sup> · Jens Twiefel<sup>3</sup> · Ludger Overmeyer<sup>2</sup> · Stefan Kaierle<sup>2,5</sup> · Jörg Wallaschek<sup>3</sup> · Bernd Breidenstein<sup>4</sup> · Bernd-Arno Behrens<sup>1,6</sup> · Malte Stonis<sup>1</sup>

Laura Budde  
l.budde@lzh.de

Jan Grajczak  
j.grajczak@lzh.de

<sup>1</sup> IPH - Institut für Integrierte Produktion Hannover gGmbH, Hollerithallee 6, 30419 Hannover, Germany

<sup>2</sup> Laser Zentrum Hannover e.V., Hollerithallee 8, 30419 Hannover, Germany

<sup>3</sup> Leibniz University Hannover, Institute of Dynamics and Vibration Research, An d. Universität 1, 30823 Garbsen, Germany

<sup>4</sup> Leibniz University Hannover, Institute of Production Engineering and Machine Tools, An d. Universität 2, 30823 Garbsen, Germany

<sup>5</sup> Leibniz University Hannover, Institute of Transport and Automation Technology, An d. Universität 2, 30823 Garbsen, Germany

<sup>6</sup> Leibniz University Hannover, Institute of Forming Technology and Machines, An d. Universität 2, 30823 Garbsen, Germany